LIMITS FOR BEAM INDUCED DAMAGE: RECKLESS OR TOO CAUTIOUS?

A. Bertarelli, V. Boccone, F. Carra, F. Cerutti, A. Dallocchio, N. Mariani,
CERN, Geneva, Switzerland
L. Peroni, M. Scapin, Politecnico di Torino, Turin, Italy

Abstract

Accidental events implying direct beam impacts on collimators are of the utmost importance as they may lead to serious limitations of the overall LHC Performance. In order to assess damage threshold of components impacted by high energy density beams, entailing changes of phase and extreme pressures, state-of-the-art numerical simulation methods are required.

In this paper, a review of the different dynamic response regimes induced by particle beams is given along with an indication of the most suited tools to treat each regime. Particular attention is paid to the most critical case, that of shock waves, for which standard Finite Element codes are totally unfit. A novel category of numerical tools, named Hydrocodes, has been adapted and used to analyse the consequences of an asynchronous beam abort on Phase 1 Tertiary Collimators (TCT).

A number of simulations has been carried out with varying beam energy, number of bunches and bunch sizes allowing to identify different damage levels for the TCT up to catastrophic failure.

THERMALLY INDUCED DYNAMIC PHENOMENA

The rapid interaction of highly energetic particle beams with matter induces dynamic responses in the impacted structure [1]. The intensity and the time scale of the response can be divided in different categories depending on several parameters, mainly deposited energy, maximum energy density, interaction duration and strength of the impacted material.

Three dynamic regimes can be identified at increasing deposited energy, namely Elastic Stress Waves, Plastic Stress Waves and Shock Waves.

Stress Waves in Elastic Domain

This regime is encountered in case of relatively low energetic impacts, when induced dynamic stresses do not exceed the material yield strength. Changes of density are negligible and pressure waves propagate at the elastic sound speed (C_0) without plastic deformation. These phenomena can be very well treated with standard implicit FEM codes (e.g. Ansys Multiphysics) [2] or even with analytical tools [3].

Stress Waves in Plastic Domain

When the dynamic stresses exceed the material yield strength, plastic stress waves appear propagating at velocities slower than elastic sound speed ($C < C_0$). The affected component is permanently deformed. Changes of density can still be considered negligible. These dynamic responses can be treated at an acceptable degree of approximation with standard implicit FEM codes [4].

Shock Waves

When the deposited energy is high enough to provoke strains and stresses exceeding a critical threshold (ε_c, σ_c), an energetic shock wave is formed propagating at a velocity higher than C_0 potentially leading to severe damages in the affected component. A shock wave is characterized by a sharp discontinuity in pressure, density and temperature across its front.

It can be shown that for metal-based material, shock waves do not appear unless changes of phase occur: if one assumes uniaxial strains, critical strains required to generate shock waves are in the range of 15% for Tungsten and 7.5% for Copper, whereas the total deformation at the melting point is in the range of 2% for both metals.

HYDROCODES

When dealing with changes of phase and significant changes of density one has to resort to a new class of wave propagation codes, called Hydrocodes. These are highly non-linear Finite Element tools, using explicit time integration schemes, developed to study very fast and intense loading on materials and structures. Hydrocodes are capable of managing very high plastic deformations at elevated strain rates, encountered in such phenomena as projectile impacts on structures, explosions or, as in our case, very short and energetic particle impacts leading to material melting. They take their name from the original assumption of pure hydrodynamic behaviour of the impacted solids; nowadays the deviatoric behaviour (responsible for material 'strength') is also taken into account, however the original name is still widely used.

As opposed to a standard, implicit FEM code, hydrocodes usually rely on complex material constitutive models, as these must be able to encompass a much larger range of densities and temperatures, including changes of phase. Strength and failure models are also more complicated as they must take into account the effects of strain rate, temperature, density change etc.

Equations of State

The Equation of State (EOS) is integrated in the hydrocode to model the behaviour of materials under any state and condition. It provides the evolution of pressure

as a function of density, temperature and energy. Most used analytical EOS are Shock, Tillotson and Mie-Gruneisen, however their application is limited since analytical modelling can describe only a single phase region of the EOS [5]. A tabular EOS can be employed to appreciate material behaviour over different phases without loss in precision. Additionally, polynomial EOS can be interpolated from tabular ones. In this work a tabular EOS has been used for Tungsten, while a polynomial EOS has been assigned to Copper.

Strength Models

To model the behaviour of materials in the extreme conditions due to shock wave propagation, an advanced yielding criterion is needed. The model must take into account, in addition to strain, the strain rate (which in case of shock waves can be as high as 10^6 s^{-1}) and the temperature (above melting point the material loses its deviatoric strength and behaves as a fluid). Most used models are Johnson-Cook, Steinberg-Guinan and Johnson-Holmquist. In the present work Johnson-Cook model has been chosen for both Tungsten and Copper.

Failure Models

On the same basis, dynamic failure models must take into account many factors such as strain, strain rate, temperature, maximum and minimum pressure, fracture toughness. In addition, failure criteria also depend on the type of failure and on the mesh used for the simulation. In our work we used Maximum Plastic Strain Failure Criterion and minimum Hydrostatic Pressure Failure Criterion (Pmin) to model the behaviour of Tungsten, while the maximum Plastic Strain Criterion was used for Copper.

Validity of Results

Hydrocodes are extremely powerful tools with capabilities steadily growing; however results must be carefully analyzed. As shown in previous paragraphs, a large set of parameters is required to correctly model the material behaviour.

Unfortunately literature data providing properties of materials of interest under extreme conditions are very scarce; besides, most of the existing information is often classified as it is drawn from military research. In addition, very few data are available for metal alloys: in this study, EOS data of pure Tungsten were used instead of Inermet 180 (95% W, 3.5% Ni and 1.5% Cu alloy) [6].

Consequently presented results are affected by uncertainties that can be fully mastered only once data obtained by direct material characterization through in-house experimental testing (e.g. in the HiRadMat facility) become available.
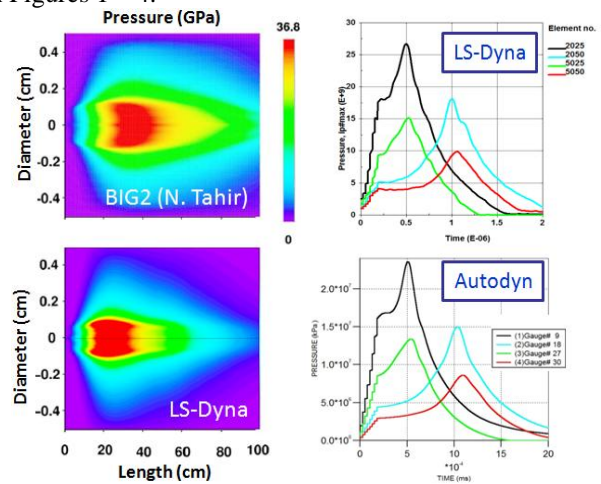
An example of comparison between numerical and experimental results, in the case of a well known material such as pure Copper, was carried out by H. Richter et al. [7].

Benchmarking between different Hydrocodes

In this work Autodyn by Ansys was extensively used, making use both of Lagrangian and Smoothed-Particle Hydrodynamics (SPH) techniques [8].

A preliminary benchmarking with other two Hydrocodes (LSDyna by LSTC, BIG-2 developed by GSI) was performed, comparing the results obtained by simulations of a cylindrical Copper sample impacted by nominal LHC bunches [9].

The good agreement between the three codes is shown in Figures 1 – 4.

Figures 1 – 4: Comparison between LSDyna, BIG-2 and Autodyn

NUMERICAL ANALYSIS OF TCT

The layout of a TCT jaw assembly is presented in Figure 5. The part of the jaw directly interacting with the beam is essentially composed of five Inermet 180 blocks, each 200 mm long. These are fixed with stainless steel screws to a support made of OFE-Cu. The Copper support is in turn brazed to cooling pipes made of Copper-Nickel alloy (90% Cu – 10%Ni), while these are brazed to a back-stiffener (made of Glidcop, a Dispersion Strengthened Copper).
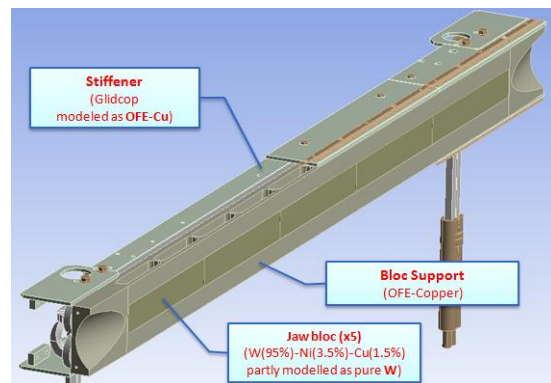

Figure 5: Jaw assembly of a TCT Collimator

Table 1 provides details about the constitutive models used for each of the relevant materials. It is worth noting that water in the cooling pipes was also included in the analysis.

Table 1: Materials models

Material	EOS	Strength model	Failure model
Tungsten [10], [11]	Tabular (SESAME)	Johnson-Cook	Plastic strain/ Hydro (Pmin)
Copper OFE [9], [10]	Polynomial	Johnson-Cook	Johnson-Cook
Stainless Steel AISI 316 [12]	Shock	Johnson-Cook	Plastic strain
Water	Shock	-	Hydro (Pmin)

Two 3D models were implemented in Autodyn:

- Full jaw with Lagrangian mesh, to study the shock-wave propagation and assess possible damage in each element of the jaw assembly;
- A short model of a single Tungsten block (200 mm) with its Copper support, along with a portion of the opposite jaw and of the stainless-steel tank cover. The Tungsten block was modelled by the SPH technique, in order to study the high-speed ejection of W particles and their impact on the tank and on the opposite jaw.

Accident scenarios

Two possible accident scenarios were identified with different degrees of severity and probability. Both scenarios are based on an asynchronous beam abort event [13].

- Single Bunch Set-Up: less severe but with higher probability. This event may occur during collimation set-up if the set-up bunch is accidentally steered at the correct phase.
- Standard multi-bunch operation: less likely with more severe consequences. In this case a series of unfortunate events must sum up:
  - Asynchronous beam abort.
  - Margin between TCDQ and TCT completely eaten up (wrong hierarchy).
  - One or more bunches steered at correct phase.

Seven cases were derived from these scenarios, with varying beam energies, intensities and emittances, conservatively assuming that all bunches have the same impact parameter (2 mm) as well as same charge (1.3 x 10^{11} p) and optical functions at TCTH.4R5B2.

It is worth noting that for multi-bunch cases, we have implicitly assumed that the density variation caused by preceding bunches is negligible: this only holds for a limited number of bunches (up to 8), before density changes become too large to be disregarded.

Relevant parameters for the studied cases are provided in Table 2 (note that energy is not scaling exactly with bunch number because of small mesh distortion during the deposition).
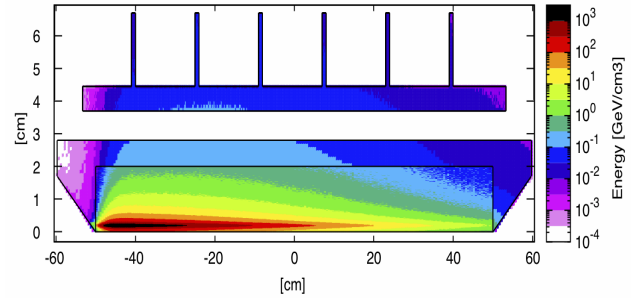
A complete FLUKA [14], [15] model of the TCT collimator was set up and full shower simulations were carried out providing the energy deposition distribution

for each case (Figure 6). These 3D maps were then loaded in the Autodyn 3D model through dedicated subroutines.

Table 2: List of accident cases.

Case	Beam Energy [TeV]	Norm. Emittance [μm rad]	N. of Impacting Bunches	Energy on Jaw [kJ]	TNT Eqv. [g]
1	3.5	3.50	1	38.6	9.2
2	5	7	1	56.2	13.4
3	5	3.5	1	56.5	13.5
4	5	1.75	1	56.6	13.5
5	5	1.75	2	111.3	26.6
6	5	1.75	4	216.1	51.6
7	5	1.75	8	429.8	**102.7**

A first, preliminary, assessment of damaged area extension can be roughly done by evaluating the molten region dimension on the Tungsten block from FLUKA maps [16].

Figures 6: Slice of the energy deposition distribution on the impacted jaw and support for Case 4 (not to scale).

In order to determine the consequence on the collimator and machine operation, three different damage levels were defined:

- Level 1 – The collimator need not be replaced. The jaw damage is limited so that an intact spare surface can be found relying on the 5th axis movement (+/- 10 mm). Permanent jaw deformation is limited.
- Level 2 - Collimator must be replaced. Damage to the collimator jaw is incompatible with 5th axis travel (damaged area diameter higher than 8 mm). Other components may also be damaged (e.g. Screws).
- Level 3 - Long down time of the LHC. Very severe damage to the collimator leading to water leakage into beam vacuum (pipe crushing, tank water circuit drilling ...).

Results

All the single-bunch cases, both at 3.5 and 5 TeV, at all emittances, fall within damage level 1. A grove is created on the two first Tungsten blocks with an extension roughly proportional to the bunch energy. The size of the damaged region is already much larger than the beam size so that no sensible difference is found when varying the beam emittance (Figure 7).
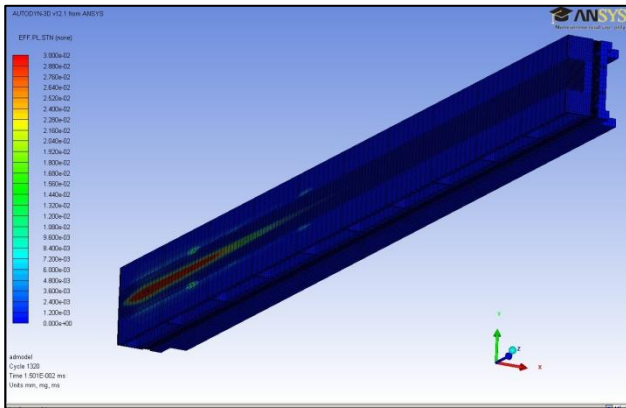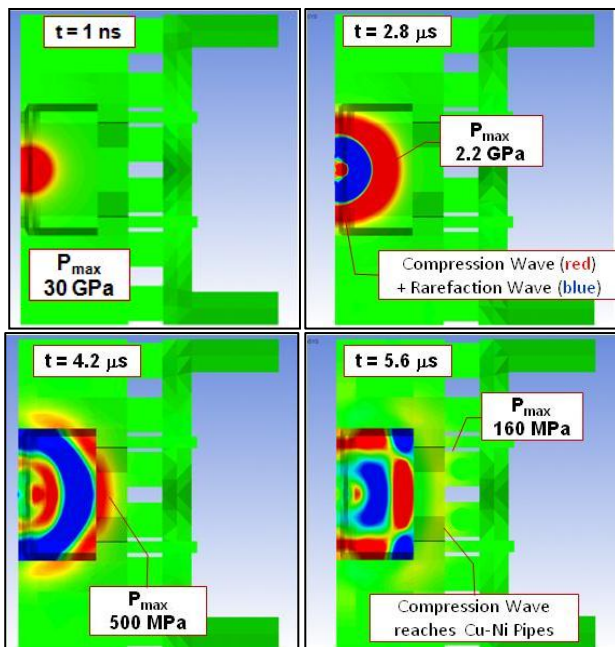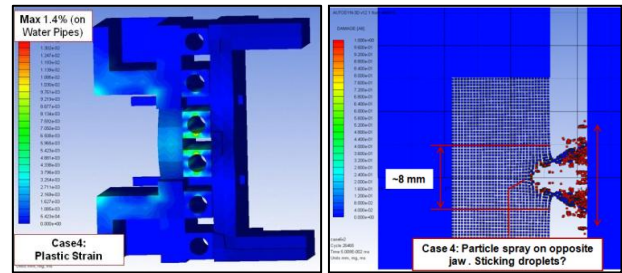
Figure 7: Extent of the damage ($\varepsilon_p > 3\%$) on Tungsten blocks (Case 4)

It is important to note that the so-called shock impedance between W and Cu, defined as $Z = \rho_0 U_s$ (with ρ_0 initial density and U_s sound speed) [17] plays a key role in limiting the damage as it confines most of the wave energy inside the Tungsten block (Figures 8-11).

It can also be observed that the jaw damage extension at 5 TeV (Case 4) is at the limit of Damage Level 2; plastic deformations on cooling pipes and screws remain limited (Figure 12); Tungsten particles are sprayed on a larger area of the opposite jaw (Figure 13): this jaw is not directly damaged; however its final flatness may be affected by possible re-solidified droplets stuck on its surface.

Figures 8–11: Case 4. Propagation of the shock wave in the jaw assembly. Note the wave is mostly reflected at the W-Cu interface, only partially transmitted to Cu Support.

Figures 12-13: Case 4. Residual Plastic strain on Cu and damage extension on W. Note particles sprayed on opposite jaw.

Cases 5 and 6 (2 and 4 bunches at 5 TeV) belong to Damage Level 2. In this case, the jaw damage extension is much larger than 8 mm and severe plastic deformations can be observed on cooling pipes ($\varepsilon_{p,max} \sim 12\%$) and screws, although visible failures are not detected. The SPH simulations show in these cases a permanent damage on the opposite jaw, provoked by the Tungsten particles impacting at elevated velocity (Figure 14).
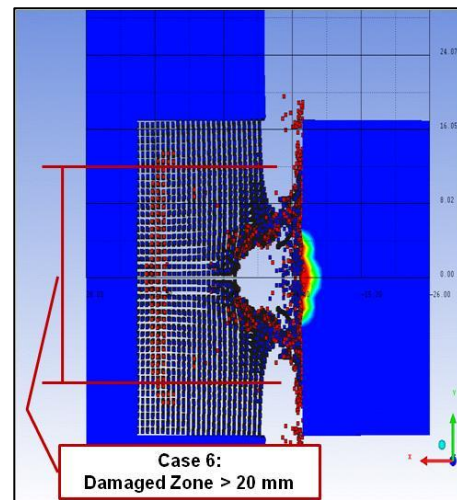

Figure 14: Case 6. High speed particle spray provoking an extended damage on the opposite jaw.

The only studied case leading to catastrophic damage (level 3) is case 7 (8 bunches at 5 TeV).

The consequences of this event are:
- High probability of water leakage due to very severe plastic deformation on pipes ($\varepsilon_{p,max} \sim 21\%$, Figure 15).
- Extended eroded and deformed zone on the W jaw.
- Projections of hot and fast solid Tungsten bullets (T ~ 2000K, $V_{max} \sim 1$ km/s) towards opposite jaw. Slower particles hit tank covers (at velocities just below ballistic limit, Figure 17);
- Risk of permanent bonding betweeen the two jaws due to the projected re-solidified material (Figure 16).
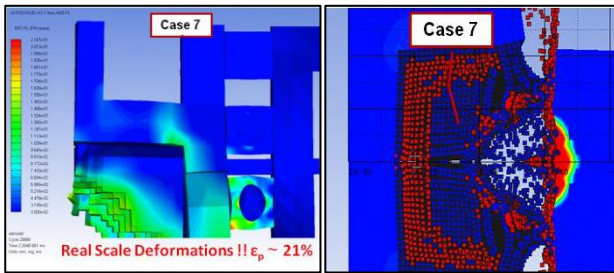
Figure 15-16: Case 7. Plastic strain and Damage extension on the two jaws (possible jaw bonding).
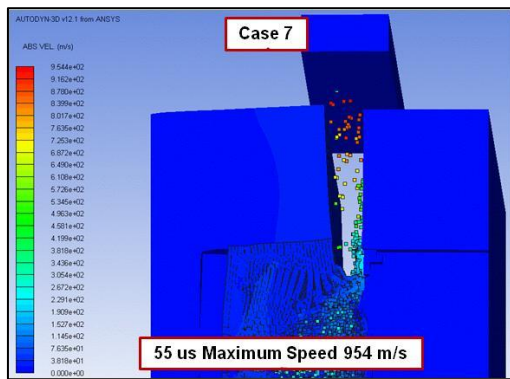

Figure 17: Particles projected towards the stainless steel tank.

CONCLUSIONS

While thermally-induced dynamic phenomena up to the melting point of metals can be reasonably well treated with standard FEM codes, advanced wave propagation codes (Hydrocodes) become necessary when changes of phase and density occur. In this paper a thorough numerical analysis of a Tertiary Collimator was carried out, relying on advanced simulation techniques applied to a complex 3D model. Several asynchronous beam abort cases were studied with different values of beam emittance, energy and intensity.

- Single-bunch accidents at 3.5 and 5 TeV induce jaw damage which does not require collimator replacement as in-situ spare surface can be found by shifting the full collimator (relying on the 5th axis).
- Multi-bunch accidents always require collimator replacement.
- Risk of very severe damage leading to long LHC downtime above four bunches (risk of water leakage detected at 8 bunches).

The most important simulation issue concerns the reliability of constitutive material models, as they are beyond commonly available data. Only specific tests in dedicated facilities (such as HiRadMat) can provide this information.

ACKNOWLEDGEMENTS

REFERENCES

[1] A. Dallocchio, G. Belingardi, T. Kurtyka, A. Bertarelli, "Study of Thermo-Mechanical Effects Induced in Solids by High Energy Particle Beams: Analytical and Numerical Methods", PhD Thesis, Politecnico di Torino, Turin 2008; CERN-THESIS-2008-140; http://cdsweb.cern.ch/record/1314219/

[2] A. Bertarelli et al., "Mechanical Design for Robustness of the LHC Collimators", PAC'05, Knoxville, May 2005.

[3] A. Bertarelli, A. Dallocchio, T. Kurtyka, "Dynamic Response of Rapidly Heated Cylindrical Rods: Longitudinal and Flexural Behaviour", Journal of Applied Mechanics, May 2008, Volume 75, Issue 3, 031010, pp. 1-13.

[4] A. Bertarelli et al. "Permanent Deformation of the LHC Collimator Jaws Induced by Shock Beam Impact: an Analytical and Numerical Interpretation", EPAC'06, Edinburgh, July 2006.

[5] M. Meyers, "Dynamic Behavior of Materials", Wiley-Interscience, 1994.

[6] Plansee CM GmbH, Inermet 180 Datasheet, http://www.plansee-cm.com/lib/lb_IT180_e.pdf

[7] H. Richter, E. Noah, H. Aiginger and K. Poljanc, "Simulation of target response due to uranium ion beam impact", Eur. Phys. J. A, Volume 42, Number 3, December 2009, Topical Issue on ENAM'08.

[8] J.A. Zukas, "Introduction to Hydrocodes", Elsevier, 2004.

[9] M. Scapin, L. Peroni, A. Dallocchio, "Thermo-mechanical modelling of high energy particle beam impacts", Proceeding ACE-X 2010, July 2010;

[10] G. R. Johnson, W.H. Cook, "A Constitutive Model and Data for Metals Subjected to Large Strains, High Strain Rates and High Temperatures", Proc. 7th Int. Symp. on Ballistics, 1983;

[11] L. Hu, P. Miller, J. Wang, "High Strain-Rate Spallation and Fracture of Tungsten by Laser-Induced Stress Waves", Materials Science and Engineering: A, Volume 504, Issues 1-2, 25 March 2009, pp. 73-80;

[12] D. Umbrello, R. M'Saoubi, J.C. Outerio, "The Influence of Johnson-Cook Material Constants on Finite Element Simulation of Machining of AISI 316L Steel", International Journal of Machine Tools & Manufacture 47 (2007): 462-470;

[13] T.Kramer et al., "Performance Studies for Protection Against Asynchronous Dumps in the LHC", IPAC'10, Kyoto, May 2010.

[14] G. Battistoni, et al., "The FLUKA code: Description and Benchmarking", Proc. of the Hadronic Shower Simulation Workshop 2006, Fermilab, AIP Conference Proceeding 896, 31-49, (2007)

[15] A. Fassò, A. Ferrari, J. Ranft, and P.R. Sala, "FLUKA: a Multi-particle Transport Code" CERN-2005-10 (2005), INFN/TC_05/11, SLAC-R-773

[16] V. Kain, W. Kutschera, R. Schmidt, "Machine Protection and Beam Quality during the LHC Injection Process", 2005, pp. 28-42;

[17] G. Ben-Dor, O. Igra, T. Elperin, "Handbook of Shock Waves, volume 1: Theoretical, Experimental and Numerical Techniques"; pp. 327-328.